Efficient parametric amplification in micro-resonators with integrated piezoelectric actuation and sensing capabilities

O. Thomas, F. Mathieu, W. Mansfield, C. Huang, S. Trolier-McKinstry et al.

Citation: Appl. Phys. Lett. **102**, 163504 (2013); doi: 10.1063/1.4802786
View online: http://dx.doi.org/10.1063/1.4802786
View Table of Contents: http://apl.aip.org/resource/1/APPLAB/v102/i16
Published by the American Institute of Physics.

Efficient parametric amplification in micro-resonators with integrated piezoelectric actuation and sensing capabilities

O. Thomas,[1,2] F. Mathieu,[3] W. Mansfield,[4] C. Huang,[4] S. Trolier-McKinstry,[4] and L. Nicu[3]
[1]*Structural Mechanics and Coupled Systems Laboratory, Conservatoire National des Arts et Métiers, 2 Rue Conté, 75003 Paris, France*
[2]*Arts et Métiers ParisTech, LSIS, 8 boulevard Louis XIV, 59046 Lille, France*
[3]*CNRS, LAAS, 7 avenue du Colonel Roche, F-31077 Toulouse Cedex 4, France*
[4]*Materials Research Institute and Materials Science and Engineering Department, The Pennsylvania State University, University Park, Pennsylvania 16802, USA*

(Received 4 February 2013; accepted 7 April 2013; published online 25 April 2013)

We report, in this work, on unprecedented levels of parametric amplification in microelectromechanical resonators, operated in air, with integrated piezoelectric actuation and sensing capabilities. The method relies on an analytical/numerical understanding of the influence of geometrical nonlinearities inherent to the bridge-like configuration of the resonators. We provide analytical formulae to predict the performances of the parametric amplifier below the nonlinearity threshold, in terms of gain and quality factor (Q) enhancement. The analysis explains how to overcome this nonlinearity threshold by controlling the drive signals. It predicts that in theory, any Q-factor enhancement can be achieved. Experimental validation demonstrates a Q-factor enhancement by up to a factor 14 in air.
 [http://dx.doi.org/10.1063/1.4802786]

Micromachined mechanical resonators are the subject of much attention due to their very high natural frequencies, large mechanical quality factor, high mechanical responsivity, and low power operation. Applications include electronic filtering and ultra-sensitive mass detection.[1–4] In those applications, one key parameter is the quality factors of the resonances, which are directly related to either the sensor sensitivity or the filter selectivity, since they govern the sharpness of the resonances.[4] When operated in air or in liquid, the quality factors dramatically decrease, thus leading to loss of performance. Several strategies have been proposed to overcome those difficulties, such as active closed loop enhancement[4,5] or parametric amplification, introduced by the pioneering work of Rugar and Grütter[6] and used for torsional microresonators.[7] More recently, this principle has been applied to micro and nano-beams driven by Lorentz forces[8] or by piezoelectric action,[9,10] to an array of microcantilevers[11] and to carbon nanotubes.[12] Pure parametric actuation has also been widely considered, for signal filtering,[13] mass sensing,[14] signal amplification,[15] or logic circuitry.[16] Geometrically nonlinear parametric amplifiers have been theoretically addressed,[17] and a strategy to tune and cancel their hardening/softening effect by active control has been proposed.[18]

This paper addresses the parametric amplification of micromachined resonators, with three main characteristics: (i) The actuation and detection are fully integrated in the resonator via the use of a single piezoelectric layer. (ii) The resonator is operated in air and we demonstrate a Q-factor enhancement of up to a factor 14 by parametric amplification. (iii) The impact of geometrical nonlinearities, which limits the devices performance, is investigated through a one degree of freedom model and numerical simulations. This leads to closed form expressions for the Q-factor enhancement and to an efficient design rule to predict and overcome the nonlinearity threshold.

It must be noted that the Q-enhancement reported in this work refers only to the artificial bandwidth decrease of resonances induced by parametric amplification. Even if this effect does not increase the ultimate mass sensing sensitivity, which is limited by thermomechanical noise,[19,20] it is of prime importance when one wants to operate the resonators into liquid or air media,[4] for which resonances as sharp as possible are sought.

The devices under study have the form of doubly clamped beams composed of several layers: a Si/SiO_2 core with piezoelectric stacks (a $PbZr_{0.52}Ti_{0.48}O_3$ (PZT) layer with top Pt and bottom Pt/Ti electrodes) at each end (Fig. 1(b)). For each device, the piezoelectric elements' lengths are 1/4 of the total length of the beams. The lengths of the two bridges selected for the experiments are 500 μm and 700 μm (Fig. 1(a)). The fabrication process has been detailed elsewhere.[21]

When electrically actuated, the piezoelectric elements attempt to contract laterally in proportion to the applied voltage $V(t)$. The mechanical action on the beam is equivalent to a concentrated moment and an axial force applied at the end of the piezoelectric element[22] (Fig. 1(c)). As a consequence, the beam is subjected to a bending action as well as a modulation of its axial tension. Since the axial tension modifies the natural frequencies of the beam, parametric driving is achievable. Parametric amplification consists of driving the beam in bending at a frequency Ω (with a voltage of amplitude V_d) and superimposing a parametric "pump" at 2Ω (of amplitude V_p), which is simply realized here with $V(t) = V_d\cos(\Omega t + \varphi) + V_p\cos 2\Omega t$. By choosing the phase difference φ, amplification of the resonance peak can be obtained when Ω is close to a natural frequency of the beam.[6,23]

A model of the microelectromechanical beams that includes the constituent layers, the change in cross-section, and the geometrical nonlinearities can be obtained by the

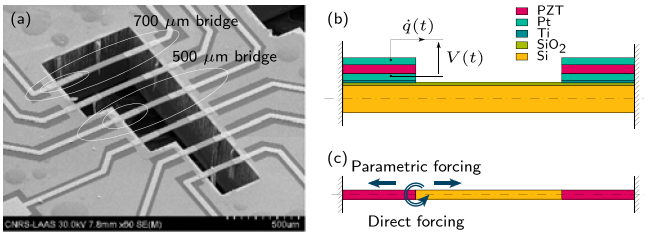

FIG. 1. (a) Scanning electron microscopy image of the devices. The two bridges selected for the experiments of Figs. 5 (500 μm) and 6 (700 μm) are shown; (b) schematic of the micro-bridges; (c) piezoelectric equivalent actuation.

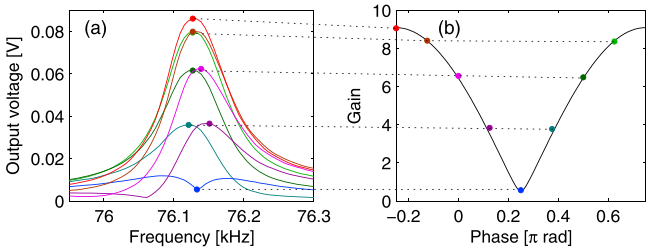

FIG. 2. (a) Experimental resonance curves of the 76.1 kHz mode of the 700 μm bridge for various phase differences φ between the direct and the parametric forcing and a constant direct forcing $V_d = 3.5$mV. (b) Gain at resonance as a function of φ. The solid line is from the analytical linear model (Eq. (2a)) and the markers are experimental data from Fig. 2(a).

finite-element method.[24] If this model is reduced to only one mode of vibration, the transverse displacement is $w(x,t) = \Phi(x)u(t)$, where $\Phi(x)$ is the deformed shape of the mode. Then, the corresponding modal coordinate $u(t)$ obeys

$$\ddot{u} + Q^{-1}\omega_0\dot{u} + \omega_0^2 u + \Gamma u^3 + \delta u \cos 2\Omega t = F_d \cos(\Omega t + \varphi), \tag{1}$$

where Q is the mechanical quality factor of the mode, ω_0 is its natural frequency, $F_d = \Theta V_d$ and $\delta = \chi V_p$ are the direct and parametric forcing amplitudes, Θ and χ are two piezoelectric coupling coefficients, and Γ is the geometrical nonlinearity parameter.[24] Because of the asymmetric beam cross-section (due to the layered structure) as well as the initial curvature of the structures at rest (stemming from residual stress), the sign of Γ is not necessarily positive, and hardening as well as softening behaviors can be obtained.[25] It must be noted that piezoelectric nonlinearities can also produce a softening effect,[26,27] due to the comparatively lower mobility of ferroelastic domain walls in thin PZT film and clamped PZT structures.[28,29] This effect is expected to be modest in this work.

The motion of the beam is monitored by measuring the electric charge $q(t)$ on the electrodes of the driving piezoelectric element (Fig. 1(b)), which is used both as an actuator and a sensor. From the model,[24] one has $q(t) = CV(t) - \chi u(t)$, where C is the capacitance of the piezoelectric layer. Since the magnitude of the "driving term" $CV(t)$ is much greater than that of the "sensing term" $\chi u(t)$, electric cancellation is done in practice, by connecting the piezoelectric layer of the vibrating beam to a second beam that is subjected to the same input voltage $V(t)$ and that is blocked from any mechanical displacement (it has not been released from the wafer during fabrication). An adjustable gain is used to cancel the driving term $CV(t)$. Then, a charge amplifier provides an output voltage proportional to $u(t)$.[21]

The parametric amplification is first considered by means of the model of Eq. (1), without geometrical nonlinearities ($\Gamma = 0$). It can be shown by a first order perturbation expansion of the solution that $u(t) = a\cos(\Omega t + \psi)$, where a is known from a closed-form expression[6,23] as a function of Ω, φ, F_d, δ, ω_0, and Q. For a non zero parametric pump ($\delta \neq 0$), the curve a as a function of Ω has a resonant shape, which depends on φ, as shown in Fig. 2(a). With $\varphi = -\pi/4$ and $\Omega = \omega_0$, the system's response under parametric excitation has a *higher amplitude* at resonance with *a narrower bandwidth*, associated with an effective quality factor $Q_{\text{eff}} = \omega_0/\Delta\omega$, where $\Delta\omega$ is the -3 dB bandwidth. This is confirmed by Fig. 2(b), where the gain at resonance $G = a(\delta \neq 0)/a(\delta = 0)$, given by Eq. (2a), is shown as a function of φ.

In the case of parametric amplification ($\varphi = -\pi/4$), the main theoretical result is that the gain $G_0 = G(\varphi = -\pi/4)$ and the quality factor enhancement Q_{eff}/Q are functions of *only one dimensionless parametric driving amplitude* $\bar{\delta} = \delta/\delta_{\text{cr}}$

$$G = \frac{\sqrt{1 + \bar{\delta}^2 - 2\bar{\delta}\sin 2\varphi}}{1 - \bar{\delta}^2}, \quad G_0 = \frac{1}{1 - \bar{\delta}}, \quad \frac{Q_{\text{eff}}}{Q} = \frac{1}{(1 - \bar{\delta})^{\eta}}, \tag{2}$$

where $\eta = 0.527$ and $\delta_{\text{cr}} = 2\omega_0^2/Q$. The gain relations ($G$ and G_0) are related to closed-form expression[6,23] while the one for Q_{eff} was obtained here by a numerical fit, with $a = f(\Omega)$ computed by numerical continuation of periodic solutions with the software MANLAB[30,31] and with Q_{eff} estimated from the -3 dB resonance bandwidth. δ_{cr} is the critical amplitude of the pure parametric forcing: if the system is driven only by parametric actuation ($F_d = 0$ in Eq. (1)), a non-zero response is obtained only if the driving amplitude δ is *above* δ_{cr}. Experimental examples of purely parametric response are shown in Figs. 5(c) and 6(c). In contrast, if $F_d \neq 0$, parametric amplification is obtained with δ *below* δ_{cr}. As δ approaches δ_{cr}, G_0 and Q_{eff} theoretically tend to infinity, so that *any quality factor* is potentially attainable by this method. With the present model without geometrical nonlinearities, if $\delta > \delta_{\text{cr}}$, the response is infinite in a frequency band around $\Omega = \omega_0$.[32]

Practically, the immovable ends of the beam in the axial direction create a nonlinear axial/bending coupling, modelled here by the cubic term of coefficient Γ. Its influence is noticeable for large amplitudes of the response, for which the resonance curve is bent toward high frequencies (if $\Gamma > 0$) or toward low frequencies (if $\Gamma < 0$). This phenomenon is observed for pure direct forcing ($\delta = 0, F_d \neq 0$), pure parametric forcing ($F_d = 0, \delta > \delta_{\text{cr}}$), and parametric amplification, as shown in Figs. 5(a), 5(c), 6(a) and 6(c). To illustrate this point, several resonance curves have been computed with MANLAB[30,31] (see Fig. 3(a)), and for each set of parameters, the gain G_0 and the effective quality factor Q_{eff} have been estimated. Figure 3 shows the result and exhibits the effect of nonlinearities: for a given value of direct forcing

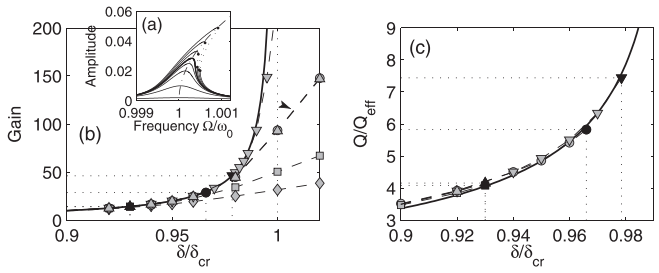

FIG. 3. (a) Resonance curves $a = f(\Omega)$ obtained by numerical computations with MANLAB,[30,31] from Eq. (1), with $Q = 500$, $F_d = 4 \times 10^{-6}, \Gamma = 1$, $\bar{\delta} \in \{0, 0.8, 0.9, 0.92, 0.93, 0.94, 0.95\}$. (b) and (c) Gain G_0 and Q-factor enhancement as a function of $\bar{\delta}$. The solid lines are from the linear model (Eqs. (2b and (2c)) and the markers $(\bigcirc, \square, \diamond, \triangledown, \Delta)$ are from the numerical results with $\Gamma = 1$, for various values of $F_d \in \{20, 50, 100, 1, 4\} \times 10^{-6}$ and $Q \in \{100, 100, 100, 500, 500\}$. The black markers and the dotted lines are associated with the geometrical nonlinearities threshold, shown in Figs. 4(c) and 4(d).

F_d, if one increases the parametric forcing δ, the response amplitude increases until a critical value above which the bending of the resonance curve is noticeable (the thick black curve of Fig. 3(a)). At this point, G_0 and Q_{eff} diverge from the theoretical formula (2) (Q_{eff} loses its physical meaning, especially when jump phenomena occur). This divergence from theory appears for a value of δ that decreases as F_d is increased.

It thus appears that the geometrical nonlinearities impose a limit on the response amplitude above which bending of the resonance curve is noticeable. Figure 4(a) illustrates this point: we denote by a_0 the amplitude of the base resonant response without parametric pump (curve 1, $F = F_d, \delta = 0$), by a_{cr} the amplitude of the critical resonant response without parametric pump above which jump phenomena appear (curve 3, $F = F_{\text{cr}}, \delta = 0$) and $a_{\max}$ the critical amplitude of the parametrically amplified resonance above

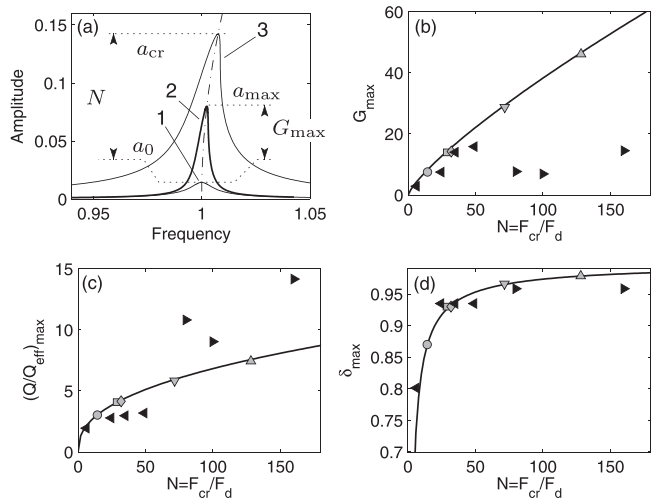

FIG. 4. (a) Various resonance curves with geometrical nonlinearities ($\Gamma = 1$, $Q = 100$). 1: base resonance curve ($F = F_d$, $\delta = 0$); 2: maximal parametrically amplified resonance below a noticeable nonlinear bending ($F = F_d, \delta = \delta_{\max}$), and 3: critical resonance curve without parametric amplification ($F = F_{\text{cr}}, \delta = 0$). (b)–(d) Maximal $G_{\max}$, Q-factor enhancement $(Q_{\text{eff}}/Q)_{\max}$, and corresponding value of $\bar{\delta}$ obtainable without noticeable bending of the resonance curve, as a function $N = F_{\text{cr}}/F_d$. Solid lines: model (Eq. (5)); grey markers $(\bigcirc, \square, \diamond, \triangledown, \Delta)$: numerical values of Fig. 3; black markers: experimental results (◀: Fig. 5;▶: Fig. 6).

which jump phenomena are observed (curve 2, $F = F_d$, $\delta = \delta_{\max}$). In the case of no parametric excitation, considering a Duffing oscillator leads to a critical amplitude at resonance $a_{\text{cr}} = \alpha\omega_0/\sqrt{Q\Gamma}$, with $\alpha = \sqrt{32\sqrt{3}/27}$.[33,34] Since $a_{\max}$ is associated with a greater quality factor than a_{cr} ($Q_{\text{eff}} > Q$), the resonance curve of the parametrically amplified resonance (curve 2) is sharper than the Duffing one (curve 3), so that the nonlinearities become noticeable for a smaller amplitude. One then observes $a_{\max} < a_{\text{cr}}$.

We note $N = a_{\text{cr}}/a_0$ the gain between the base resonant response and the critical one. We here assume that $a_{\max}$ is defined by an analogous formula, associated with Q_{eff}, so that $a_{\max} = \alpha\omega_0/\sqrt{Q_{\text{eff}}\Gamma}$. This might appear to be a crude assumption since the resonance curves have different shapes with and without parametric amplification. However, for high values of the quality factor, the curves at the resonance, near the maximum, have similar shapes. As a consequence, with this assumption, one has

$$G_{\max} = \frac{a_{\max}}{a_0} = \frac{N a_{\max}}{a_{\text{cr}}} = N\sqrt{\frac{Q}{Q_{\text{eff}}}}. \tag{3}$$

Then, following Eqs. (2b) and (2c)

$$\frac{1}{(1-\bar{\delta})^{\eta}} = \frac{Q_{\text{eff}}}{Q} = G^{\eta}, \tag{4}$$

so that

$$G_{\max} = N^{\gamma}, \quad \left(\frac{Q_{\text{eff}}}{Q}\right)_{\max} = N^{\eta\gamma}, \quad \bar{\delta}_{\max} = 1 - N^{-\gamma}, \tag{5}$$

where $\gamma = 2/(2+\eta) \simeq 0.792$ is a constant, obtained by substitution of Eq. (4) into Eq. (3).

To assess the validity of those formulas, they are compared to numerical results in Figs. 4(b)–4(d), which show $G_{\max}$ and $(Q_{\text{eff}}/Q)_{\max}$ as a function of N. The five grey markers are associated with the values of $N = a_{\text{cr}}/a_0 = F_{\text{cr}}/F_d$ from Fig. 3, where the numerical computations (with geometrical nonlinearities, $\Gamma \neq 0$) diverge from linear theory of Eqs. (2) (without geometrical nonlinearities, $\Gamma = 0$). An excellent agreement is obtained as shown in Figs. 4(b)–4(d), thus validating formula (5).

The experimental response of one mode of a 700 μm micro-bridge is shown in Fig. 5. The geometrical nonlinearities have a softening effect. It is believed to result from either the residual stresses in the micro-bridge,[35] yielding a non-zero static curvature, and/or the non-symmetrical beam cross-section.[36] Figure 5(b) leads to a critical value of the parametric pump $V_{p,\text{cr}} = 1.1235$V. Figures 5(c) and 5(d) validate the analytical gain and Q_{eff}/Q formulae (2) in the linear range, and clearly show an effect of the geometrical nonlinearities analogous to the one predicted by the numerical simulations shown in Fig. 3.

Another beam is considered in Fig. 6, where the considered mode is subjected to a nonlinear hardening effect. This probably stems from the fact that the length of the microbridge (500 μm) is shorter, so that the residual stresses lead to a less buckled state of the beam at rest. Figs. 6(c) and 6(d)

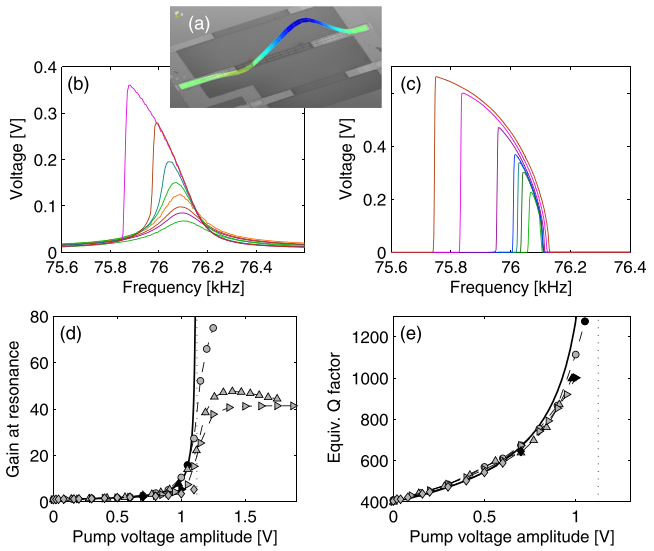

FIG. 5. Experimental results on a 700 μm micro-bridge, for a mode of resonance frequency $\omega_0/2\pi = 76.1$kHz and $Q = 400$. (a) Deformed shape measured with a laser vibrometer; (b) resonance curves for various values of the parametric pump ($V_d = 20$mV, $V_p \in \{0, 0.16, 0.3, 0.5, 0.7, 0.9, 1.1\}$V); (c) resonance curve in pure parametric driving ($V_d = 0$, $V_p \in \{1.1235, 0.127, 1.129, 1.131, 1.138, 1.155, 1.19\}$V); (d) and (e) Gain $G_{\max}$ and quality factor enhancement $(Q_{\text{eff}}/Q)_{\max}$ as a function of the parametric forcing voltage V_p. The solid lines show the theoretical formula (2) (associated with $\Gamma = 0$) and the markers stems from experiments, for various values of the direct forcing amplitude ($\bigcirc, \Delta, \triangleright, \diamond : V_d \in \{2.5, 3.5, 5, 20\}$mV). The black markers mark the threshold for geometrical nonlinearities, as shown in Figs. 4(c) and 4(d).

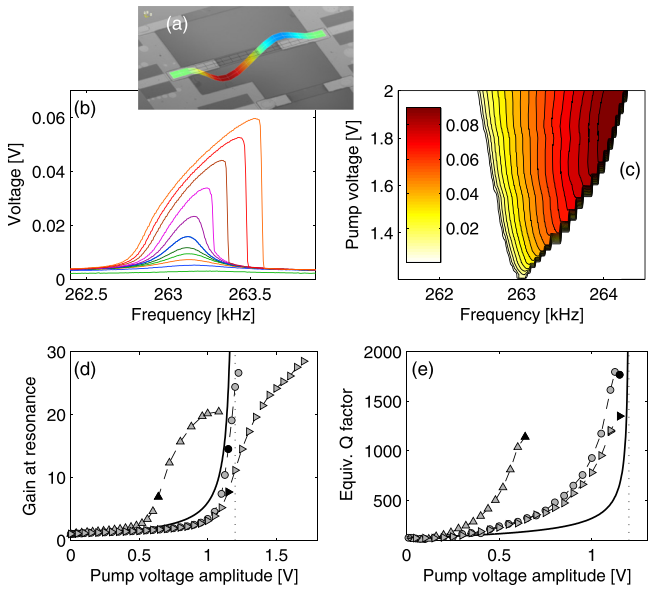

FIG. 6. Experimental results on a 500 μm micro-bridge, for a mode of resonance frequency $\omega_0/2\pi = 263.1$kHz and $Q = 125$ (see Fig. 5 for analogous details). (b) $V_d = 5$mV, $V_p \in \{0, 0.65, 0.9, 1, 1.05, 1.1, 1.15, 1.2, 1.25, 1.3, 1.35\}$V; (c) contour plot of the resonance curves in pure parametric driving ($V_d = 0$, y-axis: V_p, color levels: output voltage); (d) and (e) $\bigcirc, \Delta, \triangleright : V_d \in \{2.5, 4, 5\}$mV.

show only a qualitative agreement to the linear theory, mainly because the output electric charge response of this beam is one order of magnitude smaller than for the 700 μm beam at equivalent input voltage, so that the measured output voltages are very close to the noise floor. Thus, the tuning of the adjustable gain to cancel the parasitic electric capacitance is rendered very difficult and disturbance-prone.

The utility and the relevance of the theoretical gain and Q_{eff}/Q formulas (5) were evaluated from the experiments. The value of $V_{d,\text{cr}}$ (F_{cr}), for a given mode, was evaluated by monitoring the resonance curve *without* parametric pumping for increasing driving amplitude and estimating the one above which jumps in the resonance curve appear. Then, the same procedure was applied *with* parametric pumping (Figs. 5(b) and 6(b)). The corresponding experimental values of $N = F_{\text{cr}}/F_d$, $G_{\max}$, $(Q_{\text{eff}}/Q)_{\max}$, and $\bar{\delta}_{\max}$ lead to the black markers on Figs. 4(c) and 4(d). Good quantitative agreement is observed for the 700 μm bridge mode, thus validating the formula. For the same reasons as before, results for the 500 μm bridge are not as good. The experimental value of Γ has not been estimated, since we are interested only in the ratio $N = F_{\text{cr}}/F_d$ which does not depend on Γ (Eq. (3)).

The parametric amplification process is clearly observable in Figs. 5(b) and 6(b), with a Q-factor enhancement of 3 on the 700 μm beam and up to a factor 14 for the 500 μm beam (Figs. 5(e), 6(e), and 4(c)), in air. Following Eq. (5), since F_{cr} and δ_{cr} are fixed parameters, a given Q-factor enhancement relies only on the choice of F_d, with no theoretical limitation: the smaller F_d is, the larger the parametric amplification effect will be. In practice, the voltages V_d and V_p can be separated by several orders of magnitude (The best Q-factor enhancements were obtained with $V_d = 2.5$mV and $V_p = 1.01$V for the 700 μm beam and with $V_d = 4$mV and $V_p = 1.15$V for the 500 μm beam), which is the main limitation.

In future work, further improvements could be achieved by designing the piezoelectric layers to have coupling coefficients such that Θ is large and χ is very small (since $F_d = \Theta V_d$ and $\delta = \chi V_p$). A simple solution would be to cover the whole length of the beams with the piezoelectric layer. This might theoretically lead to $\chi = 0$ because of the clamped boundary conditions. In practice, because the boundary conditions are not ideal, it would lead to a small χ that should provide an efficient parametric amplification process. This solution has been tested,[9] but not analyzed in terms of efficiency and design.

The authors would like to thank Cédric Ayela and Isabelle Dufour from IMS Brodeaux for dynamic measurements with a Polytec MSA500 laser vibrometer as well as Bernard Legrand from IEMN Lille for fruitful discussions. The French National Agency for Research (Program ANR/PNANO 2008 and Project NEMSPIEZO "ANR-08-NANO-015") is also gratefully acknowledged for financial support. Support for the Penn State Nanofabrication Laboratory was provided in part by the National Science Foundation Cooperative Agreement No. ECS-0335765.

[1]B. Ilic, Y. Yang, and H. G. Craighead, Appl. Phys. Lett. **85**, 2604 (2004).
[2]Y. T. Yang, C. Callegari, X. L. Feng, K. L. Ekinci, and M. L. Roukes, Nano Lett. **6**, 583 (2006).
[3]V. B. Chivukula and J. F. Rhoads, J. Sound Vib. **329**, 4313 (2010).
[4]T. Alava, F. Mathieu, L. Mazenq, C. Soyer, D. Remiens, and L. Nicu, J. Micromech. Microeng. **20**, 075014 (2010).
[5]T. Manzaneque, J. Hernando-García, A. Ababneh, P. Schwarz, H. Seidel, U. Schmid, and J. L. Sánchez-Rojas, J. Micromech. Microeng. **21**, 025007 (2011).
[6]D. Rugar and P. Grütter, Phys. Rev. Lett. **67**, 699 (1991).

[7]D. W. Carr, S. Evoy, L. Sekaric, H. G. Craighead, and J. M. Parpia, Appl. Phys. Lett. **77**, 1545 (2000).
[8]R. B. Karabalin, X. L. Feng, and M. L. Roukes, Nano Lett. **9**, 3116 (2009).
[9]R. B. Karabalin, S. C. Masmanidis, and M. L. Roukes, Appl. Phys. Lett. **97**, 183101 (2010).
[10]I. Mahboob and H. Yamaguchi, Appl. Phys. Lett. **92**, 173109 (2008).
[11]Z. Yie, N. J. Miller, S. W. Shaw, and K. L. Turner, J. Micromech. Microeng. **22**, 035004 (2012).
[12]C.-C. Wu and Z. Zhong, Appl. Phys. Lett. **99**, 083110 (2011).
[13]J. F. Rhoads, S. W. Shaw, K. L. Turner, and R. Baskaran, J. Vib. Acoust. **127**, 423 (2005).
[14]W. Zhang and K. L. Turner, Sens. Actuators, A **122**, 23 (2005).
[15]R. B. Karabalin, R. Lifshitz, M. C. Cross, M. H. Matheny, S. C. Masmanidis, and M. L. Roukes, Phys. Rev. Lett. **106**, 094102 (2011).
[16]I. Mahboob and H. Yamaguchi, Nat. Nanotechnol. **3**, 275 (2008).
[17]J. F. Rhoads and S. W. Shaw, Appl. Phys. Lett. **96**, 234101 (2010).
[18]J. M. Nichol, E. R. Hemesath, L. J. Lauhon, and R. Budakian, Appl. Phys. Lett. **95**, 123116 (2009).
[19]K. L. Ekinci, Y. T. Yang, and M. L. Roukes, J. Appl. Phys. **95**, 2682 (2004).
[20]A. N. Cleland, New J. Phys. **7**, 235 (2005).
[21]F. Mathieu, F. Larramendy, D. Dezest, C. Huang, G. Lavallee, S. Miller, C. M. Eichfeld, W. Mansfield, S. Trolier-McKinstry, and L. Nicu, "Reducing parasitic effects of actuation and sensing schemes for piezoelectric microelectromechanical resonators," Microelectronic Eng. (in press) (2013).
[22]J. Ducarne, O. Thomas, and J.-F. Deü, J. Sound Vib. **331**, 3286 (2012).
[23]R. Lifshitz and M. C. Cross, "Nonlinear dynamics of nanomechanical and micromechanical resonators," in *Reviews of Nonlinear Dynamics and Complexity* (Wiley, 2008), Vol. 1, p. 52.
[24]A. Lazarus, O. Thomas, and J.-F. Deü, Finite Elem. Anal. Des. **49**, 35 (2012).
[25]In fact, a quadratic nonlinear term βu^2 should be included in Eq. (1). Not considering it here is fully justified by the concept of nonlinear modes, where an efficient one degree of freedom approximation of the dynamics around one resonance leads to a normal form without quadratic nonlinearities. (see C. Touzé, O. Thomas, and A. Chaigne, J. Sound Vib. **273**, 77 (2004) and C. Touzé and O. Thomas, Int. J. Non-Linear Mech. **41**, 678 (2006).
[26]U. von Wagner and P. Hagedorn, J. Sound Vib. **256**, 861 (2002).
[27]S. C. Stanton, A. Erturk, B. P. Mann, and D. J. Inman, J. Appl. Phys. **108**, 074903 (2010).
[28]F. Xu, S. Trolier-McKinstry, W. Ren, B. M. Xu, Z. L. Xie, and K. L. Hemker, J. Appl. Phys. **89**, 1336 (2001).
[29]F. Griggio, S. Jesse, A. Kumar, O. Ovchinnikov, H. Kim, T. N. Jackson, D. Damjanovic, S. V. Kalinin, and S. Trolier-McKinstry, Phys. Rev. Lett. **108**, 157604 (2012).
[30]B. Cochelin and C. Vergez, J. Sound Vib. **324**, 243 (2009).
[31]A. Lazarus and O. Thomas, C. R. Mec. **338**, 510 (2010).
[32]A. H. Nayfeh and D. T. Mook, *Nonlinear Oscillations* (Wiley, 1979).
[33]V. Kaajakari, T. Mattila, A. Lipsanen, and A. Oja, Sens. Actuators, A **120**, 64 (2005).
[34]N. Kacem, S. Hentz, D. Pinto, B. Reig, and V. Nguyen, Nanotechnology **20**, 275501 (2009).
[35]C. Ayela, L. Nicu, C. Soyer, É. Cattan, and C. Bergaud, J. Appl. Phys. **100**, 054908 (2006).
[36]It is known that the curvature of an arch or a shell, which breaks the symmetry of the transverse stiffness, leads, in general, to a softening nonlinear effect. In contrast, a plate or a straight beam always shows a hardening nonlinear effect.